

1 **Running title:** Spatial models for distance sampling
2 **Number of words:** ~??
3 **Number of tables:** ?
4 **Number of figures:** ?
5 **Number of references:** ?

6 **Spatial models for distance sampling data:**
7 **recent developments and future directions**

8 **David L. Miller^{1*}, Louise Burt², Eric Rexstad²,**
9 **Len Thomas².**

- 10 *1. Department of Natural Resources Science, University of Rhode Island,*
11 *Kingston, Rhode Island 02881, USA*
12 *2. Centre for Research into Ecological and Environmental Modelling,*
13 *The Observatory, University of St. Andrews, St. Andrews KY16 9LZ,*
14 *Scotland*

15 ***Correspondence author. dave@ninepointeightone.net**

16

Summary

17

Since the initial work by Hedley & Buckland (2004), there have been

18

many advances to the methodology for density surface modelling in

19

distance sampling. This review aims to describe some of the recent

20

work, in particular from spatial smoothing. We offer a comparison of

21

the various options for the practitioner as well as an examples and

22

software.

23

Keywords: Distance sampling; spatial modelling; generalized additive mod-

24

els; Poisson processes; abundance estimation.

25 Introduction

26 When surveying biological populations it is increasingly common to record
27 spatially referenced data; for example: coordinates of observations, which
28 can then be used to include information from a GIS. Mapping the spatial
29 distribution of a population can be extremely useful for practitioners, es-
30 pecially when communicating results to non-experts. Spatial models allow
31 for the vast databases of GIS data to be harnessed, allowing for interactions
32 between environmental covariates and population densities to be investig-
33 ated. Including spatial covariates into the model (for example, latitude and
34 longitude) can account for spatial autocorrelation. Recent advances in both
35 methodology and software have made spatial modelling readily available to
36 the non-specialist (e.g. Wood (2006), Rue *et al.* (2009)). Note that here we
37 use the term “spatial model” to include any model which includes spatially
38 referenced covariates, not just those which contain smooths of location.

39 This article concerns combining spatial modelling techniques with dis-
40 tance sampling (Buckland *et al.* (2001), Buckland *et al.* (2004)). Distance
41 sampling takes simple strip sampling and extends it to the case where detec-
42 tion is not certain, for example when animals are cryptic.

43 Observers travel along transect centre lines or stand at points and record
44 the perpendicular distance from the centre line or point to the object of in-
45 terest (y). These distances are used to estimate the *detection function* ($g(y)$)
46 by modelling the decrease in detectability with increasing distance from the
47 line or point. The detection function may also include animal/observer spe-
48 cific covariates (Marques *et al.* (2007)). From the fitted detection function,

the probability of detection can be calculated this gives the probability that an animal within the truncation distance is detected, which can then be used to calculate density and abundance (Buckland *et al.* (2001), Chapter 3).

In a distance sampling analysis one assumes that the objects of interest are distributed at random with respect to the lines or points (Buckland *et al.* (2001), Section 2.1) according to some process. If the objects' locations are not dependent on any spatially varying covariates (such as location, distance from coast, depth, etc) a homogenous process is assumed; so with respect to the line, the objects are distributed uniformly. It is often possible to design surveys such that this assumption holds (for example, ensuring that transect lines run perpendicular to geographical features that would attract or repel animals) or by post-stratification (Buckland *et al.* (2001), Section 3.7).

Hedley & Buckland (2004) were the first to address spatial modelling of distance sampling data, allowing for a relaxation of the homogeneity of the point process, by including a rate parameter which is a function of spatially varying covariates. Thinking of the underlying placement of the objects as an inhomogeneous point process allows us to think of the detection process as a “thinning” (Cox & Isham (1980), Section 4.3) of the process, resulting in another inhomogeneous point process. By assuming that the object placement and detection processes are independent, it is possible to separate these two processes (placement and thinning) in the likelihood.

Modelling the spatial process not only permits the use of GIS and other spatially referenced data, it also gives practitioners the freedom to use data from opportunistic surveys, for example “incidental” data arising from “eco-tourism” cruises can be included in analyses (Williams *et al.* (2006)). Al-

74 though with such non-randomly designed surveys it is still vital that there is
75 still good coverage of the area of interest.

76 The rest of the article is structured as follows: we first briefly describe
77 two methods which take the point process approach before going on to
78 describe the two-stage approach of Hedley & Buckland (2004). We then
79 describes recent advances, along with some practical advice regarding the
80 model fitting, formulation and checking. Throughout this article, a com-
81 mon, motivating data set is used to illustrate the methods. These data are
82 from a combination of several shipboard surveys conducted on pan-tropical
83 spotted dolphins in the Gulf of Mexico. These data consist of 47 observa-
84 tions of groups of dolphins. The group size was recorded, as well as the
85 Beaufort sea state at the time of the observation. Coordinates for each ob-
86 servation and depth at a series of points over the prediction area were also
87 available as covariates for the analysis. Figure 1 shows plots of the sur-
88 vey effort and observations. A complete example analysis can be found at
89 <http://www.github.com/dill/dsm/wiki/>.

90 Direct modelling of the process

91 From the point process description, two modelling procedures arise. One
92 approach is to directly model the point process, estimating the observation
93 process as the thinning of that point process (Niemi & Fernández (2010),
94 Johnson *et al.* (2010)). A second approach consists of performing a distance
95 analysis and using the fitted detection function as part of spatial model
96 (Hedley & Buckland (2004)).

97 Johnson *et al.* (2010) propose a point process-based model for distance
 98 sampling data (henceforth referred to as DSpat). They first assume that
 99 the locations of all individuals in the survey area (not just those which were
 100 observed) are a realisation of an inhomogeneous Poisson process which is a
 101 function of space. The authors then take the novel approach of allowing
 102 for separate (disjoint) regions of the survey area to have different detection
 103 functions associated with them. The sum of these detection functions is then
 104 used as a thinning of the Poisson process. The parameters are then found via
 105 standard maximum likelihood methods for point processes (see, e.g. Badde-
 106 ley & Turner (2000)). In contrast to Hedley & Buckland (2004), parameters
 107 are estimated jointly so uncertainty is incorporated. Concurrent estimation
 108 of the parameters also ensures that interactions between the thinning and
 109 underlying point process are estimated correctly. The authors also address
 110 the issue of overdispersion (commonly a symptom of animals or groups clus-
 111 tering), unmodelled by spatial covariates in a manner similar to that for the
 112 GLM (see *Recent Developments*, below, for another approach).

113 Niemi & Fernández (2010) also use Poisson processes but incorporate it
 114 into a fully Bayesian approach. Their intensity function takes the form of a
 115 product of a parametric function of the covariates and a mixture of Gaussian
 116 kernels as a spatial smooth. An appropriate degree of smoothing could be
 117 selected by putting prior distributions on the number and locations of the
 118 “knots” of the spatial smooth (the means of the Gaussian kernels) and then
 119 using the RJMCMC algorithm (Green (1995)). However, since the authors
 120 only include a single precision parameter for all of the kernels, small and large
 121 scale variation cannot both be accommodated. As in Johnson *et al.* (2010),

122 the detection function was used as a thinning of the process, although (unlike
123 DSpat) only one detection function was used across the whole region with
124 known parameters. This means that unlike DSpat (but similar to the count
125 model, above), the uncertainty in the detection function is not incorporated
126 in the spatial model.

127 Both of the above Poisson process models do not account for group size,
128 both stating that this could be included by considering a marked point pro-
129 cess (Cox & Isham (1980), Section 5.5). Both methods offer direct modelling
130 of the point process, although with some drawbacks compared to the meth-
131 odology of Hedley & Buckland (2004). It should be noted that the loss
132 of efficiency from using a two-stage approach is not large (Buckland *et al.*
133 (2004), p. 313). For these reasons, the article focuses on method of Hedley
134 & Buckland (2004) and the advances which can be applied to their method-
135 ology.

136 Density surface modelling

137 We refer to the approach of Hedley & Buckland (2004) as *density surface*
138 *modelling* (DSM), this is used as a rather general description for model-
139 ing distance sampling data using spatially referenced data. The approach
140 is incorporated into the popular software package Distance (Thomas *et al.*
141 (2010)). Rather than modelling the point process directly, DSM uses a spa-
142 tial model for the survey area using the counts, abundance (of individuals
143 or groups) or observation density as response. The principle is simple: just
144 as conventional and multiple covariate distance sampling (CDS and MCDS,

145 respectively) extend strip transect sampling to the case where detection is
 146 not guaranteed, DSM extends a spatial model for strip transects to line and
 147 point transects.

148 First, consider conducting a strip transect survey. Strips are divided into
 149 contiguous *segments* (indexed by j), which are of length s_j ; small enough
 150 such that the density does not vary a lot in the segment. For each of these
 151 segments, the number of observations (n_j) is the response and this can then
 152 be modelled as a function of spatial and environmental covariates (the \mathbf{z}_{jk}
 153 for k indexing the covariates: e.g. location, sea surface temperature, weather
 154 conditions) using a generalized linear model (GLM; McCullagh & Nelder
 155 (1989)) or generalized additive model (GAM; e.g. Wood (2006)). A GAM is
 156 used here for exposition, since the framework is more general. The covered
 157 area enters the model as an offset (the area of segment j , $A_j = 2ws_j$, where
 158 w is the truncation distance). We can model the counts as a function of
 159 covariates measured for each segment:

$$\mathbb{E}(n_j) = \exp \left[\log_e A_j + \beta_0 + \sum_k f_k(\mathbf{z}_{jk}) \right], \quad (1)$$

160 where the f_k s are smooth functions of the covariates in the GAM case
 161 (but could equally be linear functions of the covariates in the GLM case) and
 162 β_0 is an intercept term. The distribution of n_j is modelled as quasi-Poisson
 163 in Distance but other options are possible (see discussion of the Tweedie
 164 distribution, below).

166 If perpendicular distance is recorded and a CDS analysis is performed, we
167 replace A_j by $A_j \hat{P}_a$ in eqn 1, where \hat{P}_a is the probability of detection, making
168 the offset the effective area of the segment. Modelling then operates in two
169 stages, first a detection function is fitted to the distance data to obtain \hat{P}_a ,
170 then the following model is fitted:

$$\mathbb{E}(n_j) = \exp \left[\log_e A_j \hat{P}_a + \beta_0 + \sum_k f_k(z_{jk}) \right], \quad (2)$$

171 This formulation can also be used for point transects by setting $A_j = w\pi^2$,
172 $\forall j$. The above definition of the smooth terms is rather general since several
173 covariates could be included in single smooth terms via tensor products of
174 univariate bases (see Wood (2006), Section 4.1.8) or via multivariate spline
175 bases (e.g. thin plate regression splines; Wood (2003)). A typical use of a
176 bivariate spline in this setting is to smooth with respect to spatial coordinates
177 by including the centroid of the j^{th} segment or point. Basis choice for spatial
178 smooths is covered below. Note that even if spatial coordinates are not used,
179 the model is still spatial (in some sense), since the covariates used in the
180 GAM are spatially referenced.

181 If animals occur in groups or clusters, then the response variable in equa-
182 tion 2 could be either the number of groups to estimate group abundance
183 or, if group size has been recorded, then the response variable could be the
184 number of individuals per segment to estimate the individual abundance.

185 Figure 2 shows a GAM fit to the dolphin data, the top panel shows
186 predictions from a model where the counts were models as a smooth function

187 of depth, the bottom panel shows predictions where a smooth of spatial
 188 location was also included. Further discussion of the plots follows in *Practical*
 189 *advice*, below.

190 DSM WITH COVARIATES AT THE OBSERVATION LEVEL

191 The above model only considers the case where the covariates are meas-
 192 ured only at the segment/point level (which we refer to environmental or
 193 spatially-referenced covariates). Often covariates (ζ_{ij} , for individual/group
 194 i in segment j) are collected on the level of individuals (or groups); for ex-
 195 ample sex, size or observer identity. A multiple covariate distance sampling
 196 analysis (MCDS; Marques & Buckland (2003), Marques *et al.* (2007)) can
 197 then be performed and the probability of detection estimated as a function
 198 of the individual level covariates $\hat{P}_a(\zeta_i)$. Individual level covariates can be
 199 incorporated into the model by making the response the Horvitz-Thompson
 200 estimator of per-segment abundance and altering the offset term to be covered
 201 area rather than the effective area:

$$\mathbb{E}(\hat{N}_j) = \exp \left[\log_e A_j + \beta_0 + \sum_k f_k(\mathbf{z}_{jk}) \right], \quad (3)$$

202 for the multiple covariate case it is simply a case of estimating \hat{N}_j for each
 203 segment via the usual Horvitz-Thompson-type estimator (Thompson (2002):

$$\hat{N}_j = \sum_{i=1}^{n_j} \frac{1}{\hat{P}_a(\zeta_{ij})}.$$

205 Our aims in a DSM analysis are usually two-fold: estimating overall abund-
206 ance and investigating the relationship between abundance and environ-
207 mental covariates.

208 To calculate an abundance estimate for some region of interest, the ne-
209 cessary covariates (those included in the model) must be available for the
210 whole of the region, and they must also be available at the required resolu-
211 tion (using prediction grid cells that are smaller than the resolution of the
212 spatially referenced data will not have an effect on abundance/density estim-
213 ates). Having acquired the relevant data and calculated the associated areas
214 of the prediction cells, predictions can be made for the particular covariate
215 levels and abundance estimates calculated from summing predicted values
216 over the prediction grid cells.

217 As with any predictions which are outside of the range of the data, one
218 should heed the usual warnings regarding extrapolation. For example, in an
219 offshore study the effect of a continental shelf maybe cause significant issues
220 if there was not search effort on both sides of the shelf. Frequently, maps
221 of abundance or density are required and any spurious predictions can be
222 visually assessed, as well as by plotting a histogram of the predicted values.
223 A sensible definition of the region of interest is required to avoid prediction
224 outside the range of the data.

225 Abundance estimation is not the only information contained in these mod-
226 els. By looking at plots of marginal smooths of the spatially referenced
227 covariates, one can begin to understand the relationships between the covari-

228 ates and abundance. Going back to the dolphin data, we can see the effect
 229 of depth on abundance in Figure 3. There we can see that there is a large
 230 depth effect between 0 and 500m which then seems to level off (a straight line
 231 could be drawn inside the confidence band (dashed line)), indicating that the
 232 dolphins prefer water deeper than 500m. Note that the y axis in such plots
 233 is on the scale of the link function (log in this case), so care should be taken
 234 in their interpretation.

235 VARIANCE ESTIMATION

236 Estimating the variance of abundances calculated using DSM is not straight
 237 forward as uncertainty from the estimated parameters of the detection func-
 238 tion must be incorporated into the spatial model. A second consideration is
 239 that in a line transect survey, adjacent segments are likely to be highly correl-
 240 ated; failing to account for this spatial autocorrelation will lead to artificially
 241 low variance estimates and hence misleadingly narrow confidence intervals.

242 *Resampling-based methods*

243 Hedley & Buckland (2004) describe a method of calculating the variance in
 244 the abundance estimates using a parametric bootstrap, resampling from the
 245 residuals of the fitted model. The bootstrap then follows the following steps:

246 Denote the fitted values for the model to be $\hat{\boldsymbol{\eta}}$. For $b = 1, \dots, B$ (where
 247 B is the number of resamples required):

- 248 1. Resample (with replacement) the per-segment residuals, store the val-
 249 ues in \mathbf{r}_b .

- 250 2. Refit the model but with the response set to $\hat{\boldsymbol{\eta}} + \mathbf{r}_b$ (where $\hat{\boldsymbol{\eta}}$ are the
251 fitted values from the original model).
- 252 3. Take the predicted values for the new model and store them.

253 From the predicted values stored in the last step, the per-location and abund-
254 ance variance can be calculated in the usual manner. The total variance of
255 the abundance estimate can then be found by combining the variance es-
256 timate from the bootstrap procedure with the variance of the probability of
257 detection from the detection function model (using the delta method; Seber
258 (1982)). This assumes that the two components of the variance are independ-
259 ent and the method does not take into account spatial autocorrelation
260 (since the individual segments are treated as independent).

261 The above procedure assumes that there is no correlation in space between
262 segments and that residuals can be swapped around. Clearly if many animals
263 are observed in a segment then we would expect there to be a relatively high
264 level in the next segment (especially since the segments are defined after
265 the survey). A moving block bootstrap (MBB) can account for some of
266 the spatial autocorrelation in the variance estimation. The segments are
267 grouped together into overlapping blocks, (so if the block size is 5, block
268 one is segments 1, ..., 5, the second block is segments 2, ..., 6, and so on).
269 Then, at step (2) above, resamples are taken of the blocks (i.e. groups of
270 segments together) rather than individual segments within the transects.
271 Using blocks should account for some of the autocorrelation between the
272 segments, inflating the variances accordingly.

273 Williams *et al.* (2006) use a slight variation on the MBB, resampling

274 either days or trips such that the total segment length was approximately
 275 the same as that in the original survey. The authors use a jackknife (Efron
 276 (1979)), removing one day (or trip) in turn and refitting the model to the
 277 remaining data. Predictions from the fitted model could be used to calcu-
 278 late a variance and from that confidence intervals (assuming that abundance
 279 estimates are log-normally distributed; Buckland *et al.* (2001), Section 3.6)
 280 can be calculated. By calculating variances for both day and trip, the au-
 281 thors also propose an informal test of between-day correlation: if adjacent
 282 days are independent then the variance estimates for trip and day should be
 283 similar, on the other hand if the adjacent days are autocorrelated then it
 284 would be expected that the trip variance would be lower (and the confidence
 285 intervals narrower). This test could then be used to decide which of the two
 286 resampling units should be used to calculate the abundance variance (if there
 287 was evidence of autocorrelation then trip should be used). The authors also
 288 used the jackknife approach to produce maps of the study area showing how
 289 the surface changed when different parts of the data were removed.

290 The methods detailed above account only for variability in the spatial part
 291 of the model, not the uncertainty in the detection function. The above mov-
 292 ing block bootstrap can be modified to take into account detection function
 293 uncertainty by generating new distances from the fitted detection function
 294 and then re-calculating the offset by fitting a detection function to the new
 295 data. The (new) procedure works as follows:

296 For $b = 1, \dots, B$ (where B is the number of resamples required):

- 297 1. Resample (with replacement) the per-block residuals, store the values
 298 in \mathbf{r}_b .

- 299 2. Let $n_b = \hat{\boldsymbol{\eta}} + \mathbf{r}_b$, rounding to the nearest integer.
- 300 3. Generate n_b new distances from the fitted detection function, refit a
301 new detection function (with the same key function and adjustment
302 terms and selecting the number of adjustments using AIC, if required).
- 303 4. Calculate \hat{P}_a and hence a new offset.
- 304 5. Refit the spatial model (with the same covariates but allowing the
305 smoothing parameter to be selected), to the new response ($\hat{\boldsymbol{\eta}} + \mathbf{r}_b$)
306 with the new offset.
- 307 6. Take the predicted values for the new model and store them.

308 By refitting the detection function in each bootstrap resample should
309 account for the uncertainty in the detection function much much better than
310 using the delta method to combine the variances.

311 *Variance propagation*

312 Rather than using the (rather time-consuming) bootstrap methods above,
313 Williams *et al.* (2011) calculate the variance without having to refit the model
314 many times. Their method incorporates the uncertainty in the estimation of
315 the detection function into the variance of the spatial model, albeit only in
316 the case where covariates are measured at a point/segment level only. Their
317 procedure is as follows:

- 318 1. Fit the model described in eqn 2.

- 319 2. Re-fit the model with an additional random effects term. This term
320 characterises the uncertainty in the estimation of the detection function
321 (via the uncertainty of the probability of detection, \hat{P}_a).
- 322 3. Variance estimates of the abundance calculated (via the method given
323 in Wood (2006), page 245) from the model will include uncertainty
324 from estimation of the detection function.

325 We consider propagating the uncertainty in this manner not only to be more
326 computationally efficient but also preferable from a technical perspective
327 since the bootstrap methods described above do not fully account for spatial
328 autocorrelation. This failure to account for spatial autocorrelation lead to
329 overly wide confidence intervals for the abundance (or density).

330 *Visualising uncertainty*

331 There are several ways to visualise the uncertainty measures calculated above.
332 For the bootstrap methods, if at each round of the bootstrap the predicted
333 values are stored per prediction grid cell, the coefficient of variation can be
334 calculated per cell and then displayed. Figure 4 shows maps of the coefficient
335 of variation for the model which includes both location and depth covariates.
336 The top panel shows the result of running 1000 bootstrap replications in-
337 cluding detection function uncertainty as above. The bottom panel shows
338 the same plot but using the variance propagation method.

339 Recent developments

340 EDGE EFFECTS

341 Recent work (Ramsay (2002), Wang & Ranalli (2007), Wood *et al.* (2008),
342 Scott-Hayward et al (in prep) and Miller and Wood (in prep)) has highlighted
343 the need to take care when smoothing over areas with complicated boundar-
344 ies; for example, if the survey area includes rivers, peninsulae or islands. If
345 two parts of the domain (either side of a peninsula, say) are inappropriately
346 linked by the model (since the distance between the points is measured “as
347 the crow flies”, rather than “as the fish swims”) then the boundary feature can
348 be “smoothed across” leading to incorrect inference. Ensuring that a realistic
349 spatial model has been fit to the data (and, for example, that whales have
350 not been estimated to dwell on land) is essential for valid inference. The soap
351 film smoother of Wood *et al.* (2008) is particularly appealing as the model
352 jointly estimates boundary conditions for a complex study area along with
353 the “interior” smooth. This can be particularly helpful when uncertainty is
354 estimated via a bootstrap as the model helps avoid large, unrealistic predic-
355 tions which can plague other smoothers (Bravington & Hedley (2009)).

356 Even if the study area does not have a complicated boundary, edge effects
357 can still be problematic. Miller et al (in prep.) show that when using global
358 smoothers, smoothing towards the plane can cause the fitted surface to “curl-
359 up” as predictions move further away from the data. They suggest the use of
360 *Duchon splines* (a generalisation of thin plate regression splines) to alleviate
361 the problem by smoothing toward the intercept.

363 The quasi-Poisson distribution is the usual response distribution when us-
 364 ing DSM, however the Tweedie distribution offers a very flexible alternative
 365 (Candy (2004)). Tweedie distributions are a very general family of exponen-
 366 tial dispersion model. Through the parameter p , many common distributions
 367 arise; these include the normal ($p = 0$), Poisson ($p = 1$) and gamma ($p = 2$)
 368 distributions (Jørgensen (1987)). Although it is possible to optimize p , this
 369 is generally seen as unnecessary since the distribution does not change ap-
 370 preciably when p is changed by less than 0.1 (therefore trial and error is
 371 not computationally infeasible). Mark Bravington (pers. comm.) suggested
 372 plotting the square root of the absolute value of the residuals and if this
 373 plot is flat a “correct” p has been found. Additionally he suggested that a
 374 value of 1.5/1.6 for p for fisheries and 1.2 marine mammal work is generally
 375 acceptable.

376 Practical advice

377 Figure 5 shows a flow diagram of the modelling process for creating a density
 378 surface model for distance sampling data. The diagram shows which methods
 379 are compatible with each other and what the options are for modelling a
 380 particular data set.

381 In the experience of the authors, it is sensible to start with a detection
 382 function without covariates and a simple smooth of spatial location and then
 383 add in more complicated features (such as covariates in the detection func-
 384 tion, or using a soap film smoother). Model discrimination can be performed

385 for the detection function using goodness-of-fit tests (Buckland *et al.* (2004)
386 and AIC. For the spatial model, GCV score and percentage deviance ex-
387 plained are useful metrics, we also highly recommend the use of standard
388 GAM diagnostic plots. An example of such plots is given in Figure 6 along
389 with a description of their uses.

390 In the dolphin analysis presented here, we include a smooth of location.
391 This not only doubles the percentage deviance explained (27.3% to 52.7%),
392 it also allows us to account for spatial autocorrelation (in a primitive way).
393 One can see this when comparing the two plots in Figure 2 and the plot of the
394 depth in Figure 1, the plot of the smooth of depth alone looks very similar to
395 the raw plot of the depth data. A smooth of an environmental-level covariate
396 such as depth can be very useful for assessing the relationships between
397 abundance/density and the covariate, but estimates of abundance/density
398 from such models may be misleading.

399 In the analysis we have converted from latitude and longitude to metres
400 from the point (27.01, -88.3). This is because the bivariate smoother which we
401 use (the thin plate spline, Wood (2003)) is isotropic: it treats the wigglyness
402 of the smoother in each direction as equal, since a move of 1 degree in latitude
403 is not the same as a move of 1 degree in longitude, the move to meters from
404 the centre of the study area is sensible (using SI units for all measurements
405 removes the need for conversion later).

406 Discussion

407 The field is quickly evolving to allow modelling of more complex data however
408 the basic principle remains as in Hedley & Buckland (2004), albeit with
409 various additions to the modelling process. We expect to see large advances
410 two areas: temporal inferences and the handling of spatial autocorrelation.
411 These should become more mainstream as modern spatio-temporal modelling
412 techniques begin to be adopted. Petersen *et al.* (2011) provide a very basic
413 framework for temporal modelling; their model includes extra smooth terms
414 for their spatial and depth smooth terms after the construction of an offshore
415 windfarm which are included via an indicator. Spatial autocorrelation can
416 be accounted for via approaches that explicitly introduce correlations such
417 as generalized estimating equations (GEEs; Hardin & Hilbe (2003)) or via
418 mechanisms such as that of Skaug (2006), which allows observations to cluster
419 according to one of several states (e.g. “feeding” or “transit”) taking into
420 account short-term agglomerations (“hot spots”).

421 Acknowledgments

422 DLM wishes to thank Mark Bravington and Sharon Hedley for their help
423 and patience in explaining and providing code for their variance propagation
424 method and alerting him to the existence of the Markov modulated Poisson
425 process.

426 **LEN: Do we need to say something about the Navy funding me**
427 **here?**

428 References

- 429 Baddeley, A. & Turner, R. (2000) Practical maximum pseudolikelihood for spatial
430 point patterns. *Australian & New Zealand Journal of Statistics*, **42**, 283–322.
- 431 Bravington, M. & Hedley, S.L. (2009) Antarctic minke whale abundance estim-
432 ates from the second and third circumpolar IDCR/SOWER surveys using the
433 SPLINTR model.
- 434 Buckland, S.T., Anderson, D., Burnham, K.P., Laake, J.L., Borchers, D.L. &
435 Thomas, L. (2001) *Introduction to Distance Sampling*. Oxford University Press.
- 436 Buckland, S.T., Anderson, D., Burnham, K.P., Laake, J.L., Borchers, D.L. &
437 Thomas, L. (2004) *Advanced Distance Sampling*. Oxford University Press.
- 438 Candy, S. (2004) Modelling catch and effort data using generalised linear models,
439 the Tweedie distribution, random vessel effects and random stratum-by-year
440 effects. *Ccamlr Science*, **11**, 59–80.
- 441 Cox, D.R. & Isham, V. (1980) *Point Processes*. Monographs on Applied Probability
442 and Statistics. Chapman and Hall.
- 443 Efron, B. (1979) Bootstrap Methods: Another Look at the Jackknife. *The Annals*
444 *of Statistics*, **7**, 1–26.
- 445 Green, P.J. (1995) Reversible jump Markov chain Monte Carlo computation and
446 Bayesian model determination. *Biometrika*, **82**, 711–732.
- 447 Hardin, J. & Hilbe, J. (2003) *Generalized Estimating Equations*. Chapman and
448 Hall/CRC, London, UK.
- 449 Hedley, S.L. & Buckland, S.T. (2004) Spatial models for line transect sampling.
450 *Journal of Agricultural, Biological, and Environmental Statistics*, **9**, 181–199.
- 451 Johnson, D.S., Laake, J.L. & Ver Hoef, J.M. (2010) A model-based approach for
452 making ecological inference from distance sampling data. *Biometrics*, **66**, 310–
453 318.
- 454 Jørgensen, B. (1987) Exponential dispersion models. *Journal of the Royal Statist-*
455 *ical Society: Series B ...*, **49**, 127–162.
- 456 Marques, F. & Buckland, S.T. (2003) Incorporating covariates into standard line
457 transect analyses. *Biometrics*, **59**, 924–935.
- 458 Marques, T.A., Thomas, L., Fancy, S. & Buckland, S.T. (2007) Improving estimates
459 of bird density using multiple-covariate distance sampling. *The Auk*, **124**, 1229–
460 1243.

- 461 McCullagh, P. & Nelder, J.A. (1989) *Generalized Linear Models*. Chapman &
462 Hall/CRC.
- 463 Niemi, A. & Fernández, C. (2010) Bayesian Spatial Point Process Modeling of Line
464 Transect Data. *Journal of Agricultural, Biological, and Environmental Statistics*,
465 **15**, 327–345.
- 466 Petersen, I.K., MacKenzie, M., Rexstad, E., Wisz, M.S. & Fox, A.D. (2011) Com-
467 paring pre- and post-construction distributions of long-tailed ducks *Clangula*
468 *hyemalis* in and around the Nysted offshore wind farm, Denmark: a quasi-
469 designed experiment accounting for imperfect detection, local surface features
470 and autocorrelation. 2011-1.
- 471 Ramsay, T. (2002) Spline smoothing over difficult regions. *Journal of the Royal*
472 *Statistical Society. Series B, Statistical Methodology*, pp. 307–319.
- 473 Rue, H., Martino, S. & Chopin, N. (2009) Approximate Bayesian inference for
474 latent Gaussian models by using integrated nested Laplace approximations. *J.*
475 *R. Statist. Soc. B*, **71**, 319–392.
- 476 Seber, G.A.F. (1982) *The Estimation of Animal Abundance and Related Paramet-*
477 *ers*. Blackburn Pr.
- 478 Skaug, H.J. (2006) Markov Modulated Poisson Processes for Clustered Line Tran-
479 sect Data. *Environmental and Ecological Statistics*, **13**, 199–211.
- 480 Thomas, L., Buckland, S.T., Rexstad, E.A., Laake, J.L., Strindberg, S., Hedley,
481 S.L., Bishop, J.R., Marques, T.A. & Burnham, K.P. (2010) Distance software:
482 design and analysis of distance sampling surveys for estimating population size.
483 *Journal of Applied Ecology*, **47**, 5–14.
- 484 Thompson, S.K. (2002) *Sampling*. Wiley, 2nd edn.
- 485 Wang, H. & Ranalli, M. (2007) Low-rank smoothing splines on complicated do-
486 mains. *Biometrics*, **63**, 209–217.
- 487 Williams, R., Hedley, S.L., Branch, T.A., Bravington, M.V., Zerbini, A.N. & Find-
488 lay, K.P. (2011) Chilean Blue Whales as a Case Study to Illustrate Methods to
489 Estimate Abundance and Evaluate Conservation Status of Rare Species. *Con-*
490 *servation Biology*, **25**, 526–535.
- 491 Williams, R., Hedley, S.L. & Hammond, P. (2006) Modeling distribution and
492 abundance of Antarctic baleen whales using ships of opportunity. *Ecology and*
493 *Society*, **11**, 1.
- 494 Wood, S.N. (2003) Thin plate regression splines. *Journal of the Royal Statistical*
495 *Society. Series B, Statistical Methodology*, **65**, 95–114.

- 496 Wood, S.N. (2006) *Generalized Additive Models: An introduction with R*. Chapman
497 & Hall/CRC.
- 498 Wood, S.N., Bravington, M.V. & Hedley, S.L. (2008) Soap film smoothing. *Journal*
499 *of the Royal Statistical Society. Series B, Statistical Methodology*, **70**, 931–955.

Figures

Fig. 1 Top: the survey area, transect centrelines and observations with size of circle corresponding to the group size overlaid onto depth data; bottom left, histogram of observed distances with fitted detection function; bottom right, plot of distance versus group size with linear trend showing the relation between distance and group size.

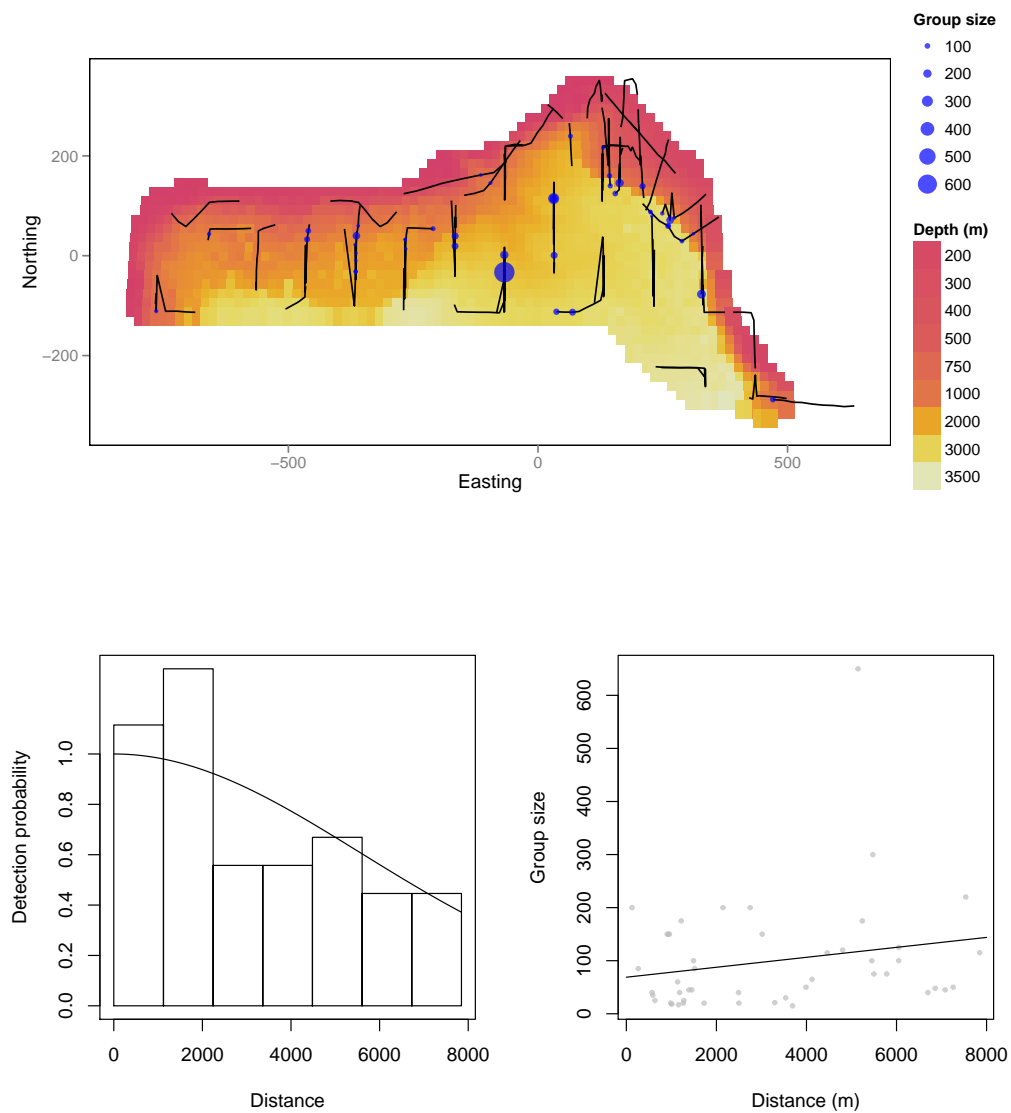


Fig. 2 Predictions for the dolphin data. Top: Predictions from the model using only depth as an explanatory variable, bottom: the model using both depth and location.

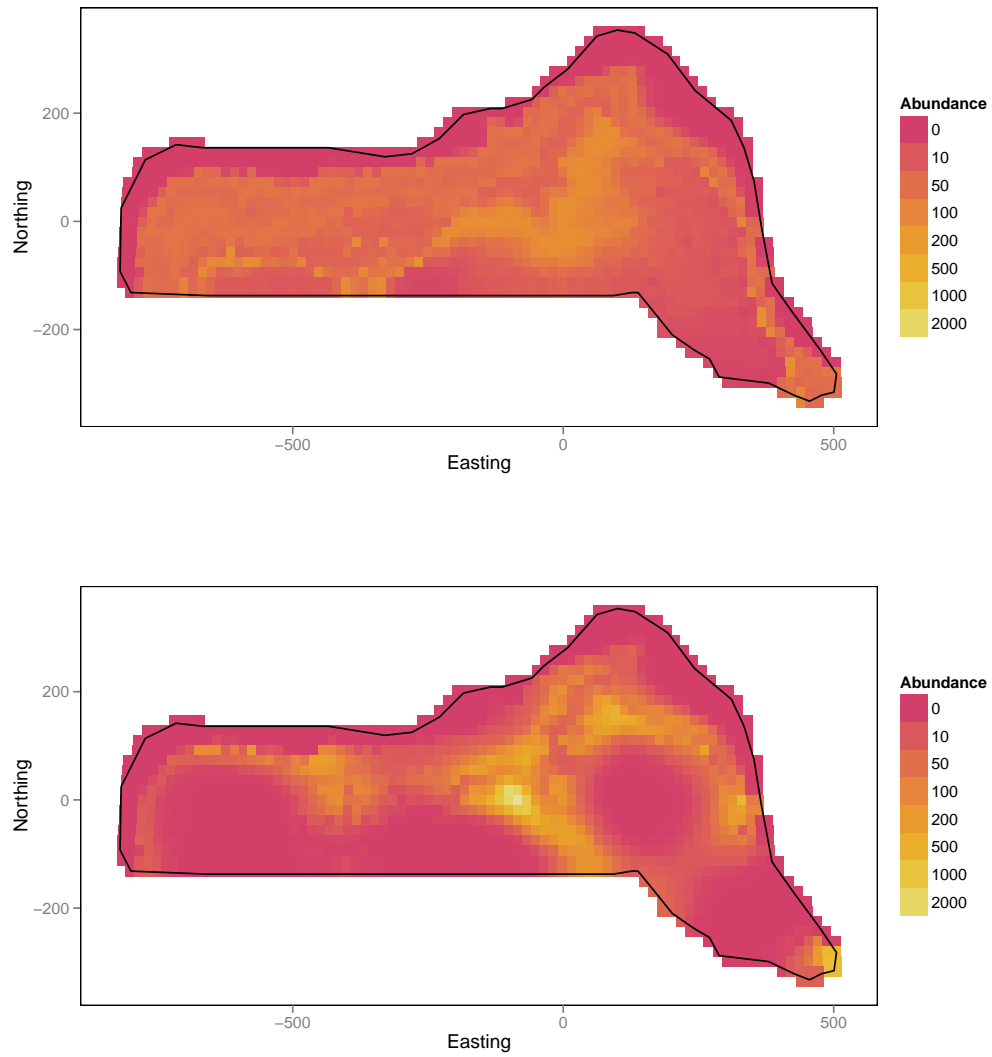


Fig. 3 Plot of the effect on the response of depth, note that it is possible to draw a straight line between 750m and 3000m within the confidence band, so the wiggles in the smooth may not be indicative of any relationship. What is clear is that there is some effect up to about 500m. The number in brackets on the y axis indicates the effective degrees of freedom of the smooth term. The rug ticks at the bottom of the plot indicate where the data were collected.

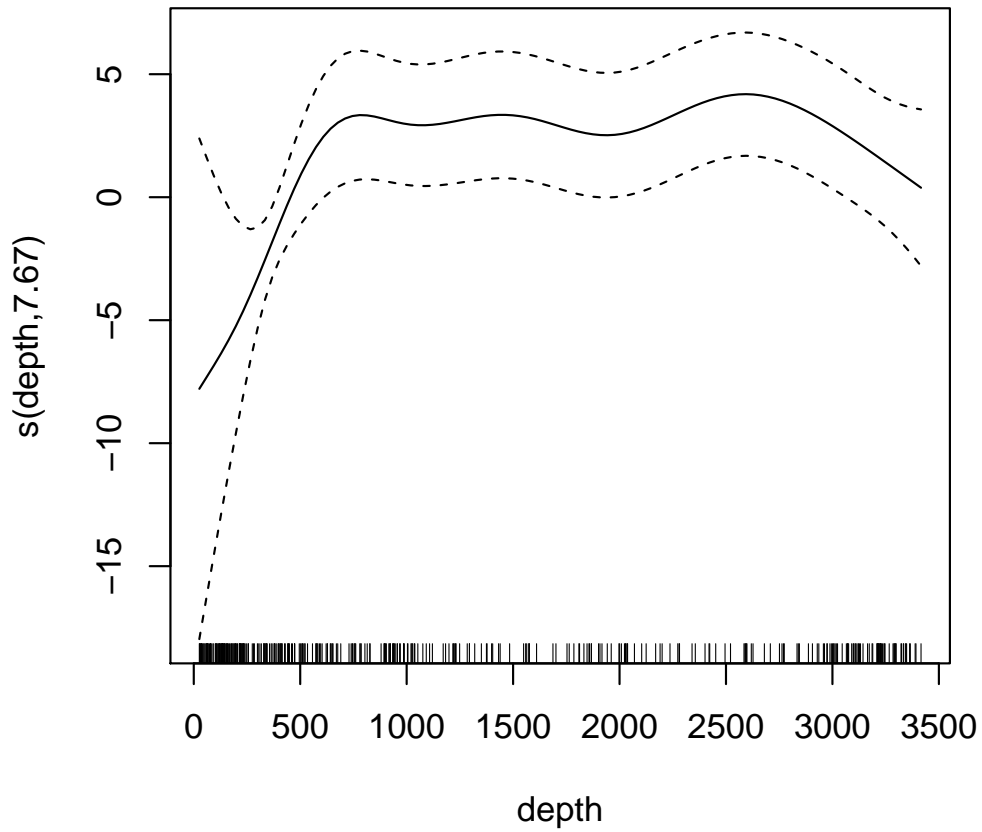


Fig. 4 Plot of coefficient of variation maps, showing the uncertainty in the fitted model. The top panel shows the estimate using the moving block bootstrap incorporating detection function uncertainty, the bottom panel shows the same plot using the variance propagation method. The bootstrap plot seems far more noisy.

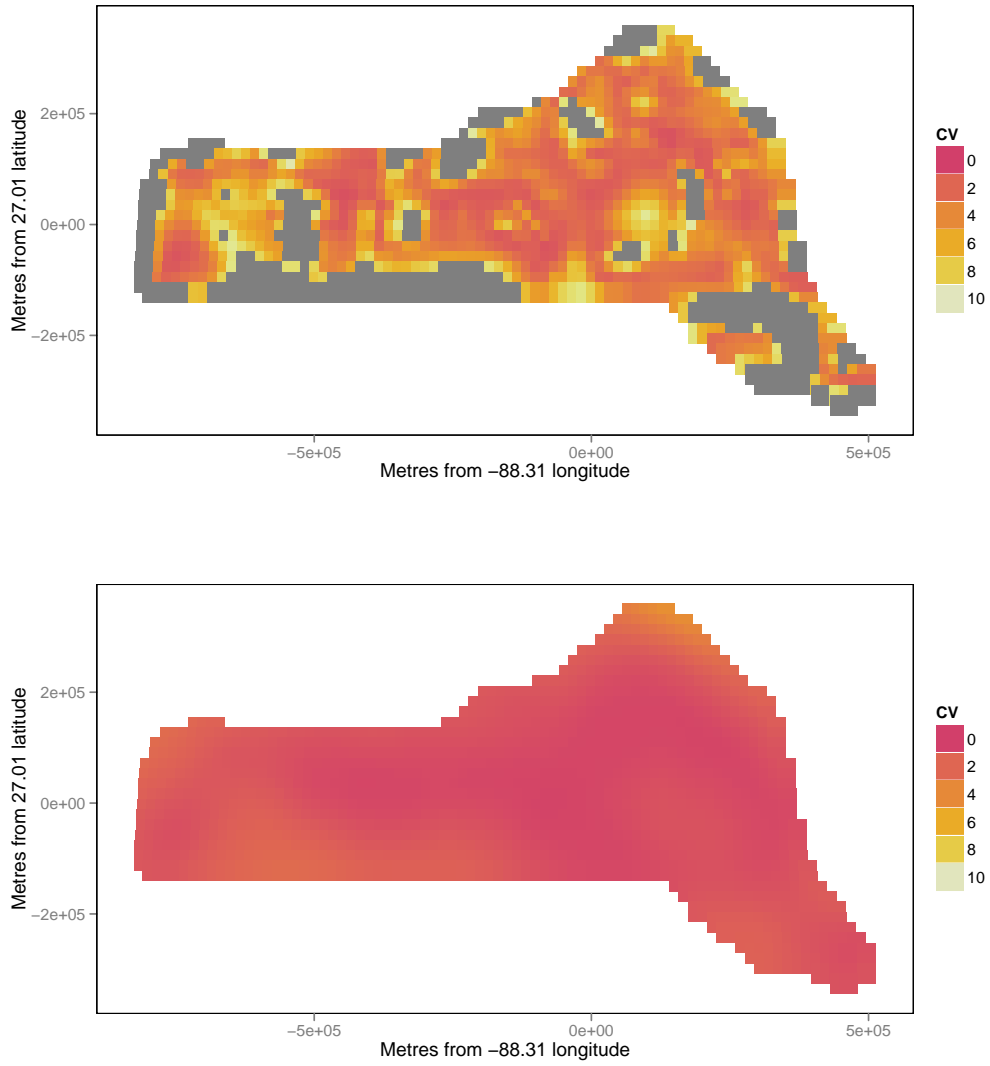


Fig. 5 Flow diagram showing the modelling process for creating a density surface model.

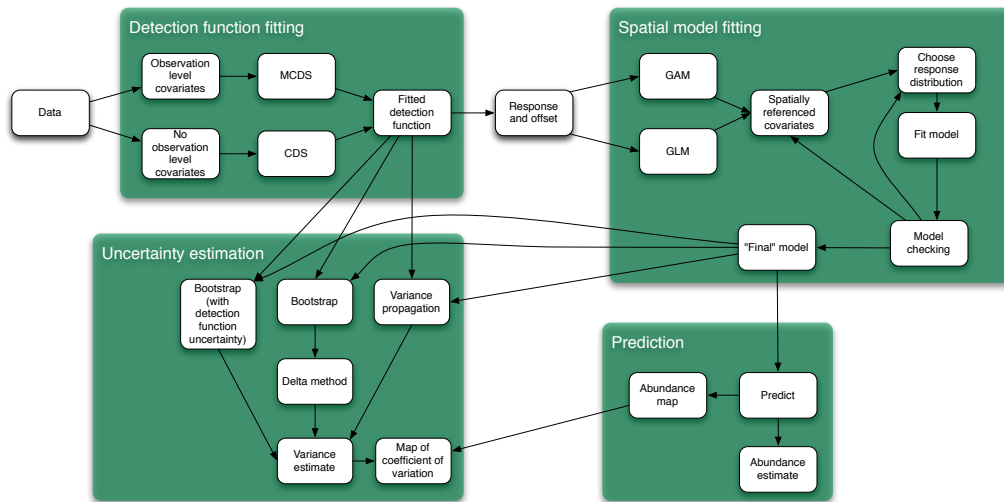


Fig. 6 Example of model diagnostics for the model which included both location and depth covariates for the dolphin data. From top left clockwise:

